

Spontaneous and Induced Ferroelectricity in the $\text{BiFe}_{1-x}\text{Sc}_x\text{O}_3$ Perovskite Ceramics

Vladimir V. Shvartsman,* Dmitry D. Khalyavin, Nikolai M. Olekhovich, Anatoli V. Pushkarev, Yuri V. Radyush, and Andrei N. Salak

High-pressure synthesis method allows obtaining single-phase perovskite $\text{BiFe}_{1-x}\text{Sc}_x\text{O}_3$ ceramics in the entire concentration range. As-prepared compositions with x from 0.30 to 0.55 have the antipolar orthorhombic $Pnma$ structure but can be irreversible converted into the polar rhombohedral $R3c$ or the polar orthorhombic $Ima2$ phase via annealing at ambient pressure. Microstructure defects and large conductivity of the high-pressure-synthesized ceramics make it difficult to study and even verify their ferroelectric properties. These obstacles can be overcome using piezoresponse force microscopy (PFM) addressing ferroelectric behavior inside single grains. Herein, the PFM study of the $\text{BiFe}_{1-x}\text{Sc}_x\text{O}_3$ ceramics ($0.30 \leq x \leq 0.50$) is reported. The annealed samples show a strong PFM contrast. Switching of domain polarity by an electric field confirms the ferroelectric nature of these samples. The as-prepared $\text{BiFe}_{0.5}\text{Sc}_{0.5}\text{O}_3$ ceramics demonstrate no piezoresponse in accordance with the antipolar character of the $Pnma$ phase. However, application of a strong enough electric field induces irreversible transition to the ferroelectric state. The as-prepared $\text{BiFe}_{0.7}\text{Sc}_{0.3}\text{O}_3$ ceramics show coexistence of ferroelectric and antiferroelectric grains without poling. It is assumed that mechanical stress caused by the sample polishing can be also a driving force of phase transformation in these materials alongside temperature and external electric field.

G-type antiferromagnetic order is due to superexchange interaction between magnetic moments of B-site Fe^{3+} ions.^[1] The weak ferromagnetic state is allowed in BFO due to Dzyaloshinsky–Morya’s interaction.^[6] However, the cycloidal modulation of the magnetic moment direction cancels the net magnetization.^[7] The high Curie (1100 K)^[8] and Neel (643 K)^[9] temperatures have motivated numerous attempts to modify the properties of BFO, keeping the large ferroelectric polarization and inducing sizable magnetization, which are important for applications.


Modification of chemical composition is the classic approach for tailoring the properties of materials. In the case of BFO, there have been many reports on substitution of Bi^{3+} by trivalent (rare-earth) or divalent (earth-alkali) cations in the full concentration range using the conventional synthesis methods.^[2,10,11] At the same time, a wide range substitution in the Fe site for bulk materials is possible only via the high-pressure synthesis (followed by quenching from 1000 to 1500 K under a pressure of 4–6 GPa). Several systems of the $\text{BiFeO}_3\text{–BiB}^{3+}\text{O}_3$ ($\text{B}^{3+} = \text{Mn}, \text{Co}, \text{Sc}$) solid solutions were prepared by this method.^[12–14] The high-pressure-synthesized materials are typically metastable at ambient pressure and show rich phase diagrams with unusual properties.

For the $\text{BiFe}_{1-x}\text{Sc}_x\text{O}_3$ system, a systematical study of the structure and magnetic properties was conducted for the entire concentration range.^[14–18] The compositions with $0 \leq x \leq 0.25$ as

1. Introduction

Bismuth ferrite, BiFeO_3 (BFO), has attracted immense attention as a rare case of a room-temperature single-phase multiferroic.^[1–3] It is classified as type-I multiferroic,^[4] in which the polar and magnetic orders appear independently. The ferroelectric order in BFO results from off-center displacements of A-site Bi^{3+} cations along $\langle 111 \rangle_{\text{pseudocubic}}$ directions,^[5] whereas the ground

V. V. Shvartsman
Institute for Materials Science and Center for Nanointegration Duisburg-Essen (CENIDE)
University of Duisburg-Essen
Universitätsstrasse 15, Essen 45141, Germany
E-mail: vladimir.shvartsman@uni-due.de

 The ORCID identification number(s) for the author(s) of this article can be found under <https://doi.org/10.1002/pssa.202100173>.

© 2021 The Authors. physica status solidi (a) applications and materials science published by Wiley-VCH GmbH. This is an open access article under the terms of the Creative Commons Attribution License, which permits use, distribution and reproduction in any medium, provided the original work is properly cited.

DOI: 10.1002/pssa.202100173

D. D. Khalyavin
ISIS Facility
Rutherford Appleton Laboratory
Chilton, Didcot, Oxfordshire OX11 0QX, UK

N. M. Olekhovich, A. V. Pushkarev, Y. V. Radyush
Scientific-Practical Materials Research Centre of NASB
P. Brovka Str. 19, Minsk 220072, Belarus

A. N. Salak
Department of Materials and Ceramics Engineering and CICECO – Aveiro Institute of Materials
University of Aveiro
Aveiro 3810-193, Portugal

synthesized under high pressure adopt the rhombohedral $R3c$ structure like that in the parent BFO. The antipolar orthorhombic $Pnma$ phase is observed in the as-prepared samples in the range of $0.30 \leq x \leq 0.65$, whereas the monoclinic $C2/c$ phase forms when $x \geq 0.70$. The $Pnma$ phase was shown to transform into other polymorphs during thermal cycling. For the composition with $x = 0.30$, annealing at $T > 475$ K results in an irreversible transformation into the rhombohedral $R3c$ phase. The compositions with $0.40 \leq x \leq 0.55$ also transform into the $R3c$ phase upon heating, but upon subsequent cooling, they undergo a reversible transition to the polar orthorhombic $Ima2$ phase. The latter phase represents a rare example of canted ferroelectricity.^[15] The monoclinic $C2/c$ compositions irreversibly transform into another orthorhombic $Pnma$ phase, which is also antipolar but is different from the aforementioned orthorhombic phase observed in the as-prepared samples with x between 0.30 and 0.60. Only for the $\text{BiFe}_{0.40}\text{Sc}_{0.60}\text{O}_3$ composition, the heating/cooling cycles with the maximum temperature up to 920 K (about the decomposition temperature) do not induce any phase transformation. This property of controlled-annealing-stimulated irreversible phase transformations is called “conversion polymorphism.”^[18]

The ferroelectric nature of the polar polymorphs with the $R3c$ and $Ima2$ symmetries was concluded based on the results of the structural studies.^[14,15] However, ferroelectricity in these materials has not actually been proven. The canonical approach to measure the polarization hysteresis loops in such high-pressure-stabilized materials was found to be inapplicable because of the relatively high conductivity of the obtained ceramics caused by the intrinsic crystal properties and the

extrinsic contributions such as amorphous intergrain phase and microcracks. This obstacle can be overcome using the piezoresponse force microscopy (PFM) method. PFM has been developed for investigation of ferroelectrics at the nanoscale and allows both the imaging of ferroelectric domains and the study of polarization switching at the local scale.^[19] The method allows to probe ferroelectricity inside a single grain. It detects piezoelectric strain induced by a strongly inhomogeneous field. Therefore, conductivity and microstructure defects of the sample are less crucial as in the case of macroscopic polarization measurements.

In this article, we report on results of the PFM studies of the $\text{BiFe}_{1-x}\text{Sc}_x\text{O}_3$ (hereafter BFSc100x) ceramics with $x = 0.3, 0.4,$ and 0.5 . It has been proven that $Ima2$ and $R3c$ polymorphs obtained by means of annealing of high-pressure-synthesized samples are indeed ferroelectric. Moreover, we show that the antipolar (antiferroelectric) state of the as-synthesized polymorphs can be converted to the ferroelectric state not only by annealing but also via application of mechanical stress or poling by an electric field.

2. Results

Figure 1 shows the topography and the PFM images of the as-prepared BFSc50 ceramics. One can see that the sample shows no true piezoresponse contrast (Figure 1b,c). Some variations of the PFM signal well correlate with peculiarities of the microstructure (grain boundaries, pores, etc.) and therefore can be considered as artifacts due to the electrostatic contribution to the PFM signal.^[19]

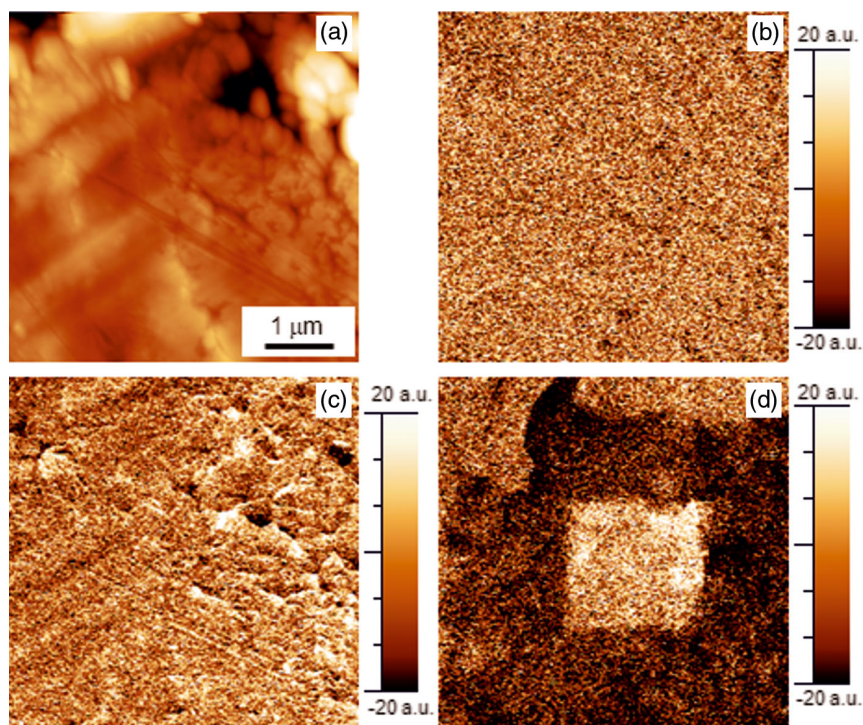


Figure 1. a) Topography, b) vertical PFM, and c) lateral PFM images of the as-synthesized BFSc50 ceramics. d) The vertical PFM image after scanning under dc voltage $U_{dc} = +50$ V (inner square) and $U_{dc} = -50$ V (outer square).

On the contrary, the annealed BFSc50 sample demonstrates the distinct piezoresponse contrast, indicating the presence of ferroelectric domains with different polarity (Figure 2b,c). Here in the vertical PFM image (Figure 2b), the dark and the bright contrasts correspond to the ferroelectric domains with up and down orientations of the out-of-plane component of polarization, respectively. In the lateral PFM image (Figure 2c), the dark and bright contrasts correspond to the left and the right directions of the in-plane component of polarization.

While existence of the domains of opposite polarity is the sufficient condition for ferroelectricity, we also conducted a polarization switching test, which is the standard procedure to confirm the ferroelectric character of a material. Specifically, we scanned a selected area of the annealed sample under a dc bias voltage applied to the PFM cantilever tip. In this experiment, the internal square was scanned under the positive bias of +50 V, whereas the outer part was scanned under the negative bias of -50 V. Figure 2d shows the PFM image of the treated area after such poling. The formation of regions with the uniform out-of-plane polarization component parallel to the direction of the bias field indicates reversal of the polarization in some domains and thus confirms the ferroelectric character of the *Ima2* polymorph of BFSc50.

Surprisingly, the similar poling experiment conducted on the as-synthesized sample (the *Pnma* polymorph) also showed the formation of regions with the nonzero piezoresponse (Figure 1d). This indicates that the piezoelectrically inactive (antipolar) state of the as-synthesized sample is transformed to the piezoactive ferroelectric state under applied electric field. It is important to note that this field-induced state was stable and persisted after the dc bias was switched off. Figure S1b, Supporting Information, shows the PFM

image of a polarized area taken 64 h after poling. No significant changes of the pattern can be seen. When the sample is heated up to 363 K, the shape of the polarized region also remains practically the same, whereas the intensity of the PFM signal decreases (Figure S1c, Supporting Information), which can be explained by a thermostimulated decay of polarization on heating.

It should be noted that some regions scanned by the dc field did not show the induced piezoresponse. Figure 3 shows the vertical PFM image of a region, where the left and the right parts were scanned under +75 and -75 V, respectively, and local piezoresponse hysteresis loops measured at different locations. Inside of the poled area (point 1), a typical ferroelectric hysteresis loop with the butterfly shape of the PFM amplitude signal and 180° PFM phase switching was observed. A similar ferroelectric hysteresis can be seen also in the initially nonpolarized region (point 2), indicating that the field-induced transformation to the ferroelectric state also occurred there. At the same time, in other locations, no hysteresis loops were observed by applying the same voltage pulse sequence. Point 3 is located in the region that was initially scanned under dc bias (-75 V) but remained piezoelectrically inactive. Neither hysteresis loop, nor change of the piezoresponse phase took place in this point through cycling the voltage between -80 and +80 V. This means that no field-induced transition occurs in this point in the limit of the applied field. We can conclude that the transformation from the antipolar to the polar state in the as-synthesized BFSc50 ceramics is spatially inhomogeneous. As the material under study is polycrystalline, one can assume that the threshold field value required for such a transition depends on an angle between the direction of the field and the crystallographic axis of the grain.

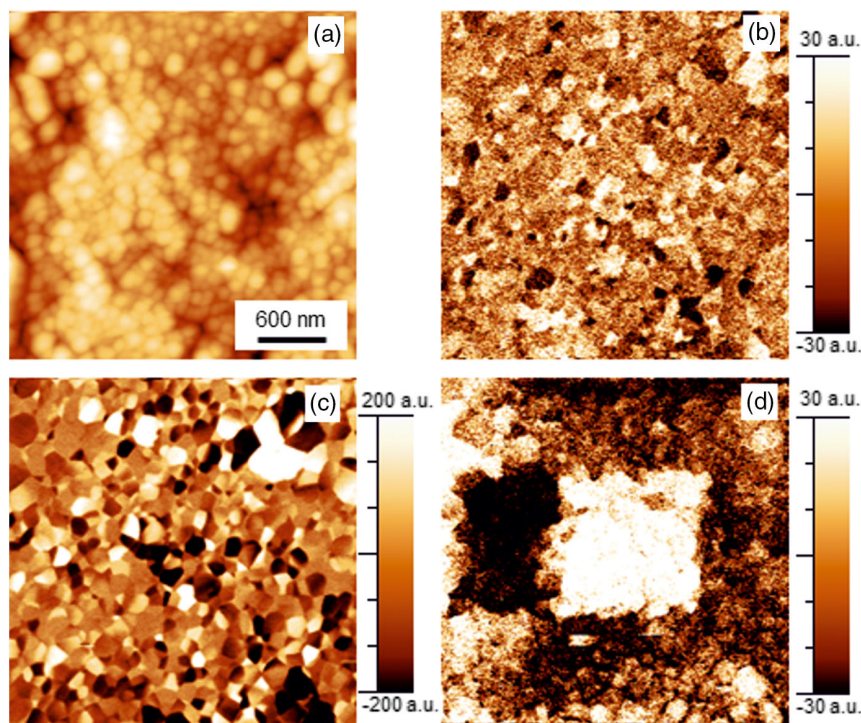


Figure 2. a) Topography, b) vertical PFM, and c) lateral PFM images of the annealed BFSc50 ceramics. d) The vertical PFM image after scanning under dc voltage $U_{dc} = +50$ V (inner square) and $U_{dc} = -50$ V (outer area).

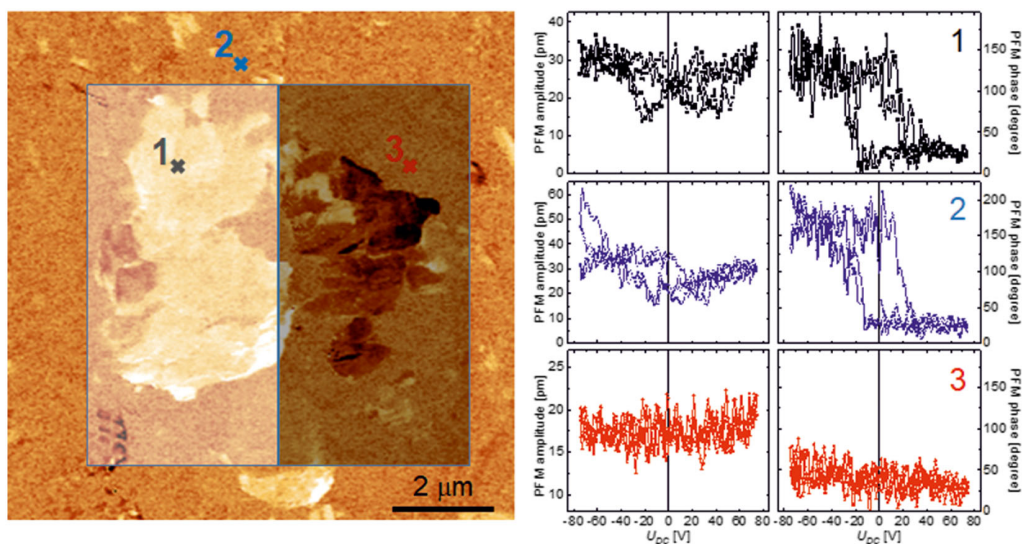


Figure 3. (left) Vertical PFM image of the as-synthesized BFSc50 ceramics after the dc poling by ± 75 V. The PFM amplitude (middle) and phase (right) hysteresis loops taken in the indicated points.

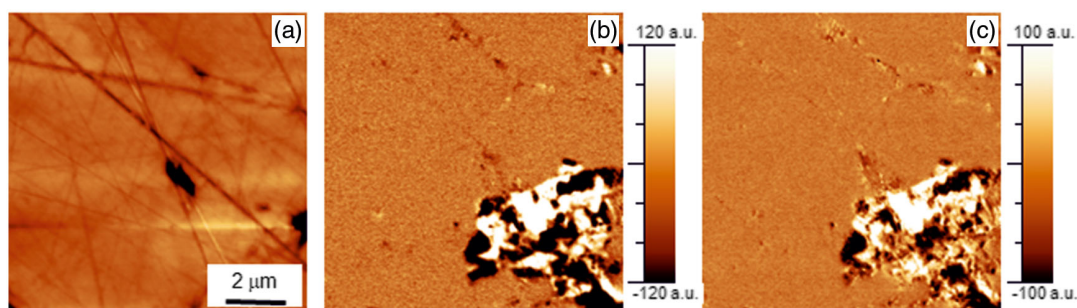


Figure 4. a) Topography, b) vertical PFM, and (c) lateral PFM image of the as-synthesized BFSc40 ceramics.

Figure 4 shows the topography and the PFM images of the as-prepared BFSc40 ceramics. As it is expected for the antipolar *Pnma* phase, most of the area is not piezoactive. However, some grains manifest a distinct PFM signal. In the as-prepared BFSc30 ceramics, the area occupied by piezoactive regions is larger and reaches $\approx 50\%$ of the total studied area (**Figure 5b**). Thus, for both as-prepared BFSc40 and BFSc30 samples, we can conclude on the coexistence of antipolar and polar phases. The amount of the polar (ferroelectric) phase increases significantly with decrease in Sc content.

According to the structural data, the BFSc30 sample exhibits the transition to the polar rhombohedral phase at 475 K.^[14] We compared the vertical PFM images of the same area of the as-synthesized BFSc30 sample taken at room temperature (**Figure 6a**) and after in situ annealing at 560 K (**Figure 6b**). One can see that the relative area of the piezoactive phase increases with annealing, indicating temperature-induced transformation to the ferroelectric state. For the sample annealed (ex situ) at 600 K, only the piezoactive phase was detected (**Figure 5d**). Similar to the case of the as-synthesized BFSc50 ceramics, scanning under a dc bias resulted in polarization of initially nonpolar regions of the as-prepared BFSc30 ceramics (**Figure S2**, Supporting Information).

3. Discussion

The obtained PFM data indicate that the annealed BFSc ceramics are in the ferroelectric state, showing domains of different polarity that can be switched by an applied electric field. This is in agreement with their polar *Ima2* or *R3c* symmetry. The as-synthesized BFSc50 ceramics is not piezoactive, which correlates well with its antipolar symmetry. In contrast, both the as-synthesized BFSc40 and BFSc30 ceramics show a coexistence of the nonpiezoactive (antipolar) and piezoactive (ferroelectric) regions. However, according to the X-ray diffraction (XRD) data,^[14,18] the only bulk structural phase detected in these ceramics is the antipolar *Pnma*. To explain the “spontaneous” formation of the ferroelectric regions, the following should be noted. First, the PFM collects the signal from a small volume around the contact point between the nanometer-sized tip and the sample. This provides the high spatial resolution of the method, but also makes it the surface sensitive. This means that the measured PFM signal corresponds to the response of the subsurface volume with a maximum thickness of 100–200 nm. Second, preparation of the sample for PFM measurements requires polishing of the sample surface. This procedure causes a mechanical stress that

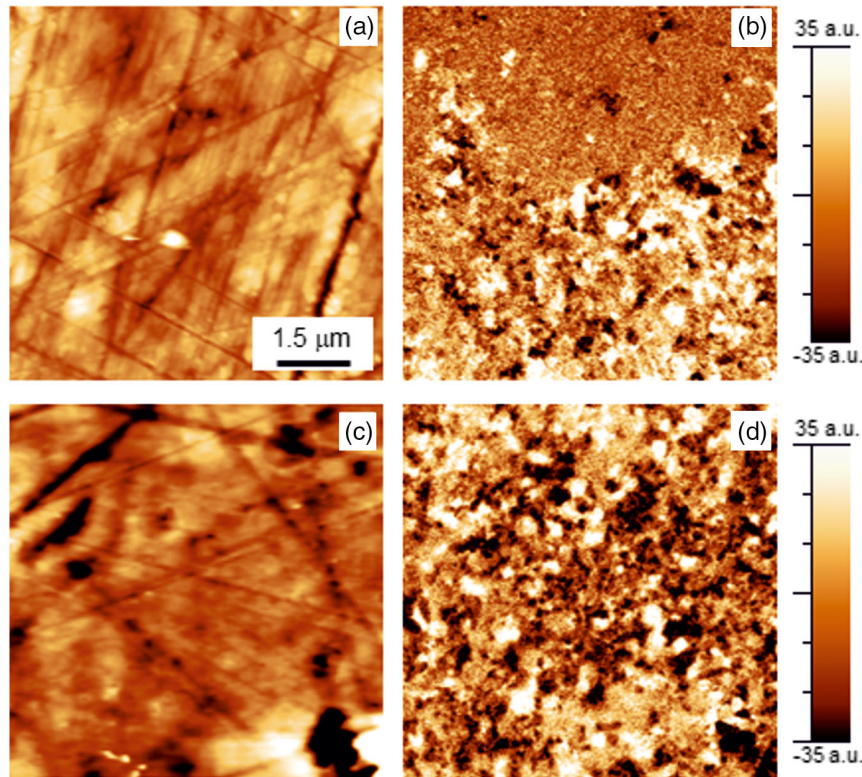


Figure 5. a) Topography and b) vertical PFM of the as-synthesized BFSc30 ceramics. c) Topography and d) vertical PFM of the annealed BFSc30 ceramics.

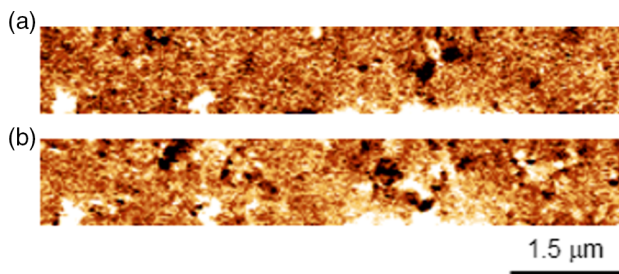


Figure 6. Vertical PFM of the as-synthesized BFSc30 ceramics a) before and b) after in situ annealing at 560 K.

can be sufficient to induce and stabilize the ferroelectric state at least in the subsurface layer.

Quenching after high-pressure synthesis allows to obtain the phases that are thermodynamically unstable or metastable at ambient conditions. The recent first-principle studies of Bi-based perovskite oxides showed that these compounds manifest a large variety of metastable phases with close energy values.^[20] The high degree of polymorphism is related in part to the lone electron pair of the Bi^{3+} ion, that attains a lobe-shape form by overlapping with oxygen orbitals, and possibility to accommodate those lobes in different combinations of polar and antipolar displacements, which lead to many local energy minima. For both BiFeO_3 and BiScO_3 , the $R3c$ phase has the lowest energy minimum, but the energy of the local minimum corresponding to the $Pnma$ phase is only 28 and 10 meV per formula unit higher, respectively.^[20] Relatively low stability of the $Pnma$ phase is

confirmed by its irreversible transformation into the polar $R3c$ phase (BFSc30) or $Ima2$ phase (BFSc50) upon annealing. The annealed BFSc40 sample shows a mixture of the $R3c$ and the $Ima2$ phases.^[16] According to the phase diagram of the $\text{BiFe}_{1-x}\text{Sc}_x\text{O}_3$ series,^[18] the temperature required to initiate transformation to the $R3c$ phase decreases from 650 K for BFSc50 to 380 K for BFSc30.

It is known that mechanical stress exerted during polishing may shift the thermodynamic balance and modify the domain structure.^[21] Therefore, we assume that this mechanical stress drives a transition into the state corresponding to the deeper energy minimum in the materials under study. For the BFSc30 sample, the boundary between the $Pnma$ and $R3c$ phases is only 100 K above room temperature.^[14] Therefore, the energy brought in by mechanical polishing might be enough to induce a partial transformation of the surface layers into the ferroelectric $R3c$ phase detected by PFM. For the BFSc40 ceramics, the $Pnma \rightarrow R3c$ phase transformation occurs at 430 K.^[14] Correspondingly, only a few ferroelectric grains are observed in the polished sample by PFM. However, in the BFSc50 sample, the $Pnma$ phase is more stable (until 650 K) and a higher energy is required to bring the system from this state to the state with a lower local minimum. Therefore, the polishing of BFSc50 sample resulted in no transition from the antipolar state.

Canonical antiferroelectrics are distinguished by so-called double-polarization hysteresis loops, manifesting a reversible transition into the ferroelectric state under an electric field above a certain threshold value. When the field is removed, the material

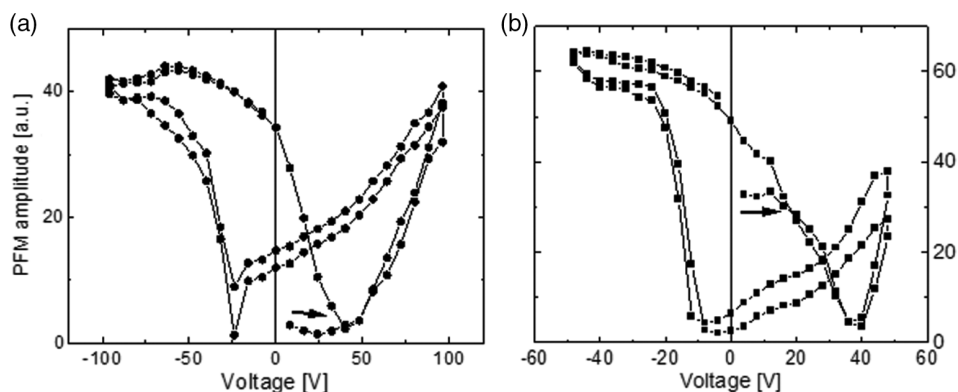


Figure 7. a) Local PFM amplitude hysteresis loop taken in an antiferroelectric grain of the as-synthesized BFSc40 ceramics. b) A hysteresis loop taken in a ferroelectric grain is shown for comparison. Arrows indicate the direction of voltage change at the beginning of measurements.

turns back into the antiferroelectric state below another threshold field. In the case of the as-prepared ceramics under study, the transition is irreversible. The induced ferroelectric state remains after the electric field is removed and does not decay either by time exposure or by heating up to 470 K (this temperature is still well below the Curie temperature). This means that similarly to the impacts of temperature or mechanical stress, electric field also drives the transition from the antipolar state to a more stable ferroelectric state. **Figure 7a** shows an example of the local piezoresponse hysteresis loops taken inside an antipolar (nonpiezoactive) grain of the as-synthesized BFSc40 ceramics. The PFM response remained initially close to zero and started increasing only above a threshold voltage of ≈ 40 V. By further sweeping of the voltage, the butterfly-like hysteresis loop typical of ferroelectrics was observed. We found that this threshold voltage value is distributed in a broad range of 15–50 V, depending on the location. Such a big scattering is not surprising for polycrystalline materials, as the value of the critical field inducing the transition to the ferroelectric state depends on the angle between the field direction and local orientation of the crystallite. Based on the phase diagram, one can also expect that for the same grain orientation, the critical field for the BFSc30 ceramics should be lower than that for the BFSc50 ceramics. However, it could not be unequivocally confirmed in the PFM experiment.

It should be mentioned that the electric field-induced irreversible antiferroelectric–ferroelectric transition has also been observed in the as-prepared antipolar orthorhombic phase of a related compound, $\text{BiFe}_{0.5}\text{Mn}_{0.5}\text{O}_3$.^[22]

4. Conclusion

PFM was demonstrated to be an efficient tool to test ferroelectricity in the materials with defect microstructures and/or high conductivity. Using this method, we have proved the ferroelectric nature of the polar polymorphs *Ima2* and *R3c* of the $\text{BiFe}_{1-x}\text{Sc}_x\text{O}_3$ perovskites obtained by annealing of their high-pressure-synthesized ceramics. The as-prepared antipolar *Pnma* polymorph is not piezoactive but can be irreversibly transformed into the ferroelectric state. A strong enough external driving force like heat (annealing), mechanical stress (polishing), or

electric field (poling) is capable of inducing ferroelectricity in these materials.

Obtained results together with data of earlier magnetic studies^[15–17] confirm the true multiferroic character of the $\text{BiFe}_{1-x}\text{Sc}_x\text{O}_3$ solid solutions. The BFSc30 composition is of particular interest. It shows not only coexistence of ferroelectric and magnetic order at room temperature, but also has the Néel temperature (≈ 380 K) close to room temperature.^[16] This allows one to expect a sizable magnetoelectric effect and makes this material interesting for application both in bulk and in thin-film forms.

5. Experimental Section

Ceramic samples of the $\text{BiFe}_{1-x}\text{Sc}_x\text{O}_3$ series with $x = 0.3, 0.4,$ and 0.5 were prepared using the high-pressure synthesis. Details of the samples preparation can be found in the study by Salak et al.^[23] Both the as-synthesized and the annealed samples of each composition were studied. Annealing was conducted at 870 K for 4 h. The phase content and structural parameters of the samples were controlled by XRD and neutron diffraction, as described in other studies.^[14–18]

Before the PFM measurements, one side of the plate-shaped sample was polished. The opposite side was electroded with silver paste.

The PFM measurements were carried out using a commercial atomic force microscope setup MFP-3D, Asylum Research. Cantilevers Multi 75E-G with Pt–Ir-coated tip (tip apex radius: 50 nm, resonant frequency about 70 kHz, spring constant about 3 N m^{-1}), Budget Sensors, were used. The probing voltage with the amplitude of $U_{ac} = 3–5$ V and frequency of $f_{ac} = 300$ kHz was used. The local piezoresponse hysteresis loops were measured using the switching spectroscopy PFM mode. The obtained data were analyzed using Gwyddion 2.47 software.

Supporting Information

Supporting Information is available from the Wiley Online Library or from the author.

Acknowledgements

The research done in University of Aveiro was supported by the project CICECO-Aveiro Institute of Materials, UIDB/50011/2020 & UIDP/50011/2020, financed by national funds, through the Portuguese Foundation for Science and Technology/MCTES.

Open access funding enabled and organized by Projekt DEAL.

Conflict of Interest

The authors declare no conflict of interest.

Data Availability Statement

Research data are not shared.

Keywords

bismuth ferrite, high-pressure synthesis, multiferroics, perovskite ceramics, piezoresponse force microscopy

Received: March 31, 2021

Revised: June 17, 2021

Published online: August 2, 2021

-
- [1] G. Catalan, J. Scott, *Adv. Mater.* **2009**, *21*, 2463.
- [2] J. Wu, Z. Fan, D. Xiao, J. Zhu, J. Wang, *Progr. Mater. Sci.* **2016**, *84*, 2013.
- [3] S. R. Burns, O. Paull, J. Juraszek, V. Nagarjan, D. Sando, *Adv. Mater.* **2020**, *32*, 2003711.
- [4] D. Khomskii, *Physics* **2009**, *2*, 20.
- [5] F. Kubel, H. Schmid, *Acta Cryst.* **1990**, *B46*, 698.
- [6] A. M. Kadomtseva, A. K. Zvezdin, Yu. F. Popov, A. P. Pyatakov, G. P. Vorob'ev, *JETP Lett.* **2004**, *79*, 705.
- [7] I. Sosnowska, T. Peterlin-Neumaier, E. Steichele, *J. Phys. C: Solid State Phys.* **1982**, *15*, 4835.
- [8] Yu. E. Roginskaya, Yu. Ya. Tomashpol'skii, Yu. N. Venevtsev, V. M. Petrov, G. S. Zhdanov, *Sov. Phys.-JETP* **1966**, *23*, 47.
- [9] S. V. Kiselev, R. P. Ozerov, G. S. Zhdanov, *Sov. Phys. Dokl.* **1963**, *7*, 742.
- [10] J. Silva, A. Reyes, H. Esparza, H. Camacho, L. Fuentes, *Integr. Ferroelectr.* **2011**, *126*, 47.
- [11] D. C. Arnold, *IEEE Trans. Ultrason. Ferroelectr. Freq. Control* **2015**, *62*, 62.
- [12] M. Azuma, H. Kanda, A. A. Belik, Y. Shimakawa, M. Takano, *J. Magn. Mater.* **2007**, *310*, 1177.
- [13] M. Azuma, S. Niitaka, N. Hayashi, K. Oka, M. Takano, H. Funakubo, Y. Shimakawa, *Jpn. J. Appl. Phys.* **2008**, *47*, 7579.
- [14] A. N. Salak, D. D. Khalyavin, E. Eardley, N. M. Olekhovich, A. V. Pushkarev, Yu. V. Radyush, A. D. Shilin, V. V. Rubanik, *Crystals* **2018**, *8*, 91.
- [15] D. D. Khalyavin, A. N. Salak, N. M. Olekhovich, A. V. Pushkarev, Yu. V. Radyush, P. Manuel, I. P. Raevski, M. L. Zheludkevich, M. G. S. Ferreira, *Phys. Rev. B* **2014**, *89*, 174414.
- [16] E. L. Fertman, A. V. Fedorchenko, E. Cižmár, S. Vorobiov, A. Feher, Y. V. Radyush, A. V. Pushkarev, N. M. Olekhovich, A. Stanulis, A. R. Barron, D. D. Khalyavin, A. N. Salak, *Crystals* **2020**, *10*, 950.
- [17] E. L. Fertman, A. V. Fedorchenko, V. A. Desnenko, V. V. Shvartsman, D. C. Lupascu, S. Salamon, H. Wende, A. I. Vaisburd, A. Stanulis, R. Ramanuskas, N. M. Olekhovich, A. V. Pushkarev, Yu. V. Radyush, D. D. Khalyavin, A. N. Salak, *AIP Adv.* **2020**, *10*, 045102.
- [18] D. D. Khalyavin, A. N. Salak, E. L. Fertman, O. V. Kotlyar, E. Eardley, N. M. Olekhovich, A. V. Pushkarev, Y. V. Radyush, A. V. Fedorchenko, V. A. Desnenko, P. Manuel, L. Ding, E. Cižmár, A. Feher, *Chem. Commun.* **2019**, *55*, 4683.
- [19] V. V. Shvartsman, A. L. Kholkin, in *Multifunctional Polycrystalline Ferroelectric Materials: Processing and Properties*, (Eds.: L. Pardo, J. Ricote), Springer, Dordrecht, Netherlands **2011**.
- [20] A. Singh, V. V. Singh, E. Canadell, J. Íñiguez, O. Diéguez, *Phys. Rev. Mater.* **2018**, *2*, 104417.
- [21] M. F. Wong, K. Zeng, *J. Am. Ceram. Soc.* **2011**, *94*, 1079.
- [22] D. Delmonte, F. Mezzadri, E. Gilioli, M. Solzi, G. Calestani, F. Bolzoni, R. Cabassi, *Inorg. Chem.* **2016**, *55*, 6308.
- [23] A. N. Salak, D. D. Khalyavin, A. V. Pushkarev, Yu. V. Radyush, N. M. Olekhovich, A. D. Shilin, V. V. Rubanik, *J. Solid State Chem.* **2017**, *247*, 90.